Supplementary Information

N-Phenylfluorubine: One Functional Dye – Chromophor, Fluorophor, Electron-Acceptor and More

D. M. Gampe[a], S. Schramm[a], M. Kaufmann[a], H. Görls[b] and R. Beckert[a]*

[a] *Friedrich Schiller University Jena, Institute of Organic and Macromolecular Chemistry, Humboldtstraße 10, 07743 Jena (Germany).*
E-mail: rainer.beckert@uni-jena.de
Website: http://www.agbeckert.uni-jena.de/
[b] *Friedrich Schiller University Jena, Institute of Inorganic and Analytical Chemistry, Humboldtstraße 8, 07743 Jena (Germany)*

New Journal of Chemistry, 2016

Content

1 General Methods

Solvents for UV-Vis and emission spectroscopy were of analytical grade and bought from Sigma–Aldrich. ^{1}H and ^{13}C NMR and the corresponding correlation spectra were recorded on Bruker AC-250 (250 MHz), AC-300 (300 MHz) and AC-400 (400 MHz) spectrometers. Chemical shifts (δ) are given relative to solvents. UV-Vis data for the compounds were collected with a PerkinElmer LAMBDA 45 UV-Vis spectrometer and emission spectra were measured with a Jasco FP 6500 instrument. Elemental analysis was carried out with a Leco CHNS- 932 instrument. Mass spectra were measured either with a Finnigan MAT SSQ 710 (EI)

or a MAZ 95 XL (ESI) system. Crystal structure determination: The intensity data were collected on a Nonius KappaCCD diffractometer, using graphite-monochromated Mo-Kα radiation. Data were corrected for Lorentz and polarization effects; absorption was taken into account on a semi-empirical basis using multiple-scans.[1] The structure was solved by direct methods (SHELXS[2]) and refined by full-matrix least squares techniques against Fo2 (SHELXL-97[2]). All hydrogen atoms were located by difference Fourier synthesis and refined isotropically. MERCURY was used for structure representations.[3] TLC materials were from Merck (Polygram SIL G/ UV254, aluminum oxide 60 F254). The material for column chromatography was also obtained from Merck (silica gel 60, 0,04 - 0,063 mm). The quantum yields were measured against fluorescein (Φ_F = 0.91 E mol^{-1} in 1 M NaOH solution) and rhodamine 6G (Φ_F = 0.95 E mol^{-1} in EtOH) as the fluorescence standards.[4] The pH values of the UV-Vis titration experiments were measured with a VWR pHenomenal MU6100H. The cyclovoltammetric measurements were performed at a Metrohm Autolab PGSTAT30 potentiostat. in 0.1 M solution of $TBAPF_6$ in THF (**3**), THF+1 drop of Tfa (pH ≈ 2.5) for $\mathbf{3H^+}$, THF/Tfa: 5:1 for $\mathbf{3H_2^{2+}}$ and DMF+1 spatula NaH for $\mathbf{3^-}$ (concentrations: 1×10^{-4} M) on a graphite working electrode with a scanning speed of 50 mV s^{-1}, platinum was used as counter and Ag/AgCl as the reference electrode. The data were calibrated externally versus ferrocen/ferrocenium.

2 Spectroscopy

2.1 Solvatochromism

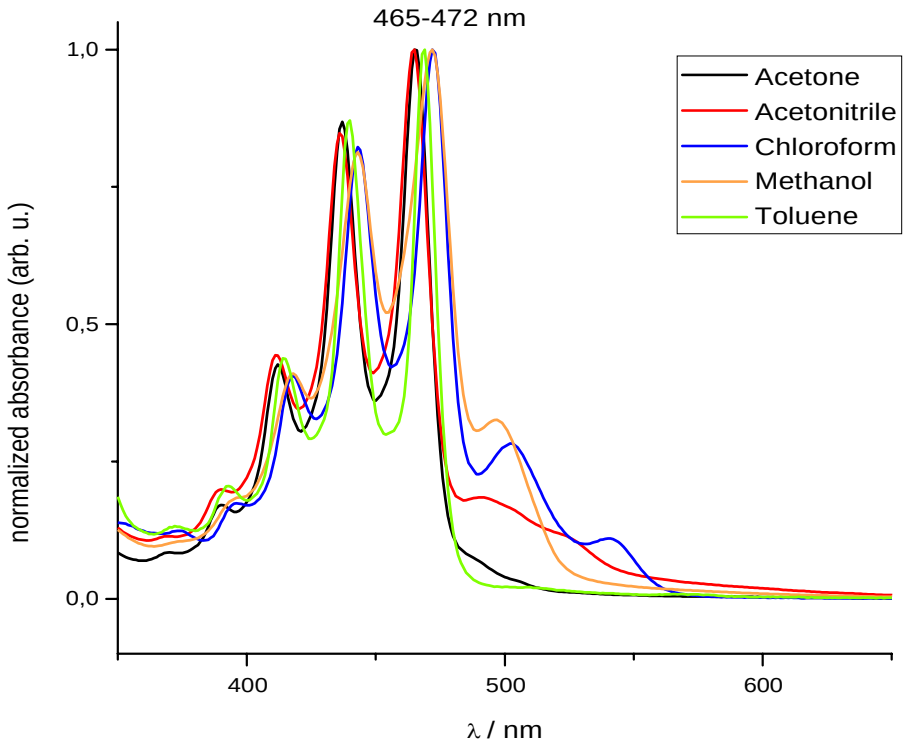

Figure S1: UV-Vis spectra of **3** in different solvents, shoulders at λ ≈ 500 nm through protolysis due to the solvent.

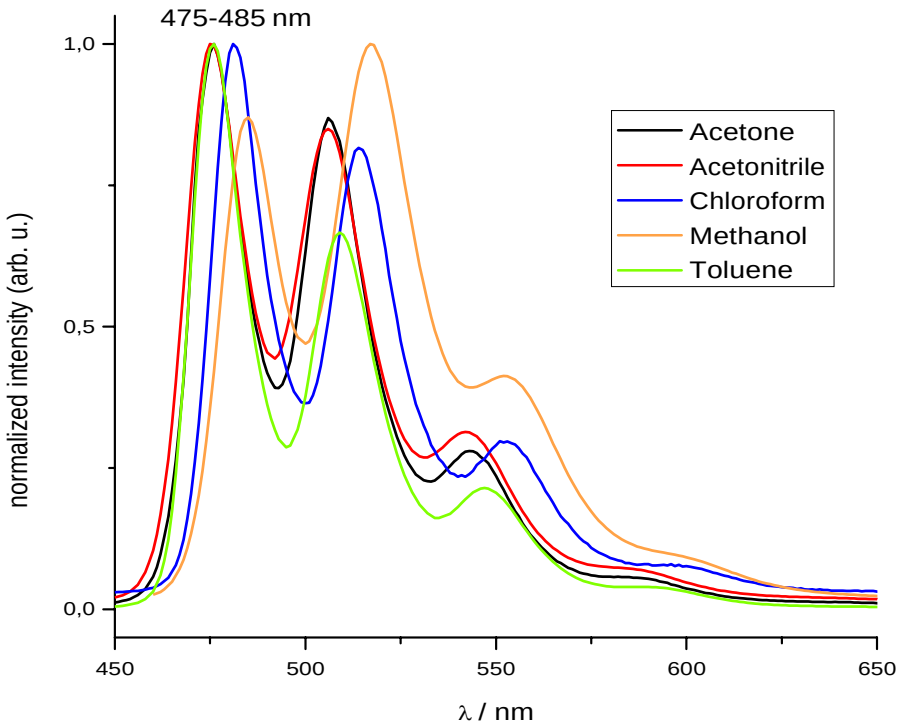

Figure S2: Fluorescence emission spectra of **3** in different solvents.

2.2 Titration

As depicted exemplarily in Figure S3 and Figure S5, the biologically relevant pK_a values were estimated via UV-Vis titration. The absorbance of an appropriate maximum was plotted against the corresponding pH, like depicted in Figure S4 and Figure S6. After this, the titration curve was fitted by a sigmoidal function, which was differentiated to give the pK_a at the corresponding maximum.

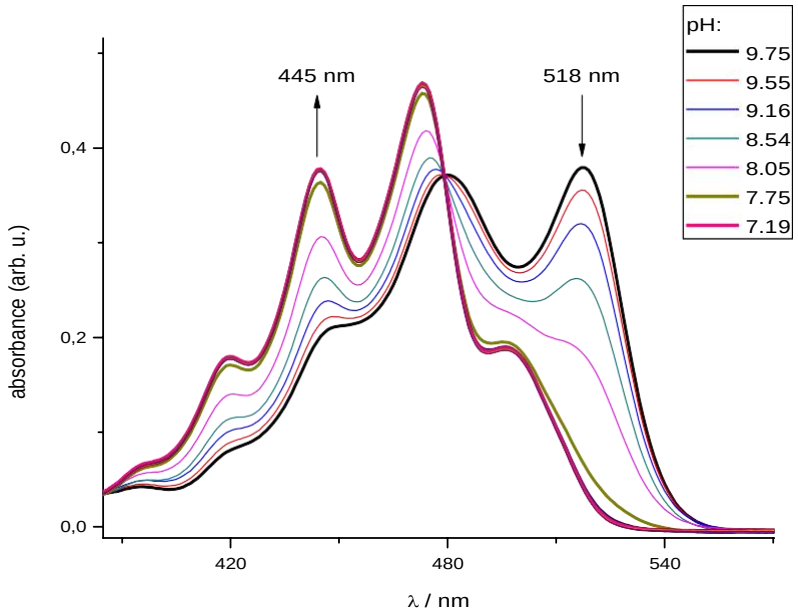

Figure S3: UV-Vis titration of an alkaline MeOH/H_2O/0.1 M NaOH (1:1:1) of **3** with 0.1 M HCl (starting with **3**$^-$to **3**, at pH = 9.75 to pH = 7.2).

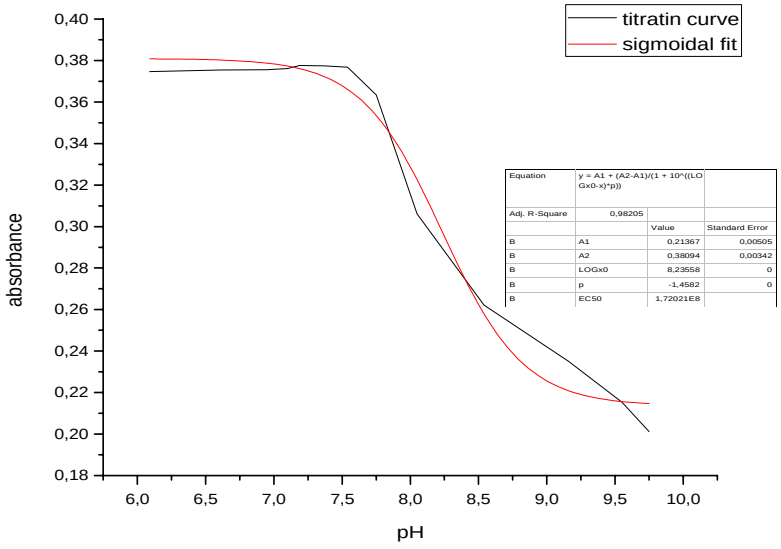

Figure S4: Sigmoidal fit of the titration curve (absorbance at λ = 445 nm against pH).

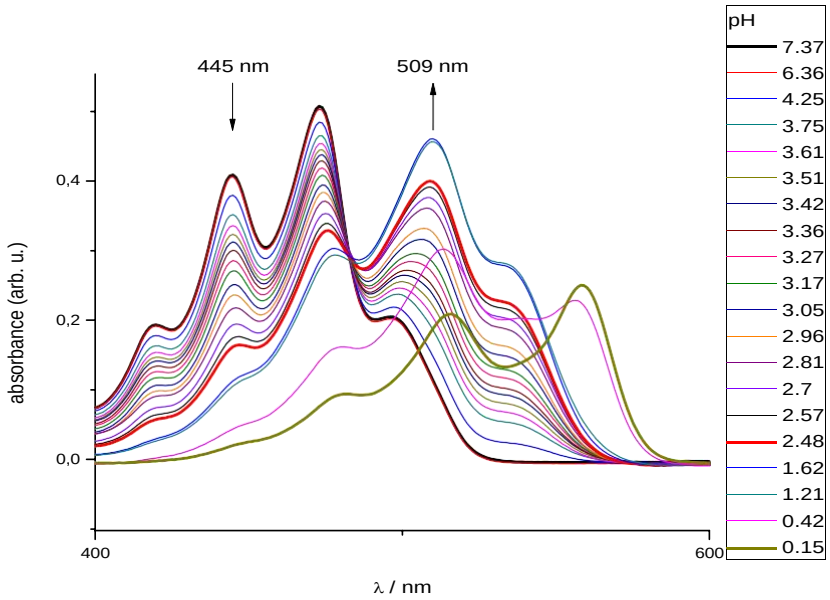

Figure S5: UV-Vis titration of a MeOH/H_2O (1:2) solution of **3** with 0.1 M HCl (starting with **3** to $\mathbf{3H^+}$ and $\mathbf{3H_2}^{2+}$)

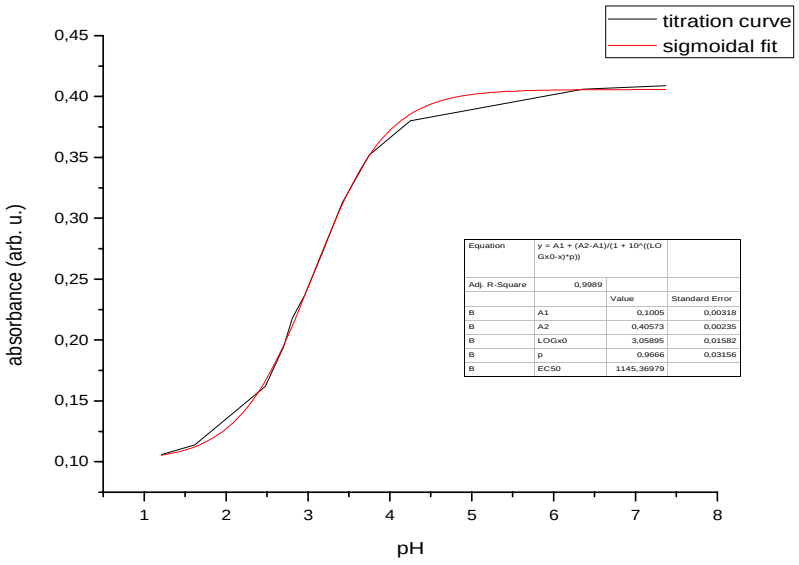

Figure S6: Titration curve of **3** to $\mathbf{3H^+}$ and the sigmoidal fit (absorbance at λ = 445 nm against pH).

2.3 CV-measurements

The CV of the neutral species of compound **3** is depicted in Figure S7. As we described in the publication, new signals were observed within the CV after the first oxidation wave (marked by arrows). For the explanation of the additional signals within the CV of fluorubine **3** we assume the mechanism as depicted in Scheme S1 and like Dunsch and co-workers postulated in 1996.[5] These signals could not be observed by measuring $\mathbf{3^-}$ as deprotonated species (see Figure S10), which furthermore explains the postulated mechanism and the presence of a stabilized radical or follow-up reactions of the latter.

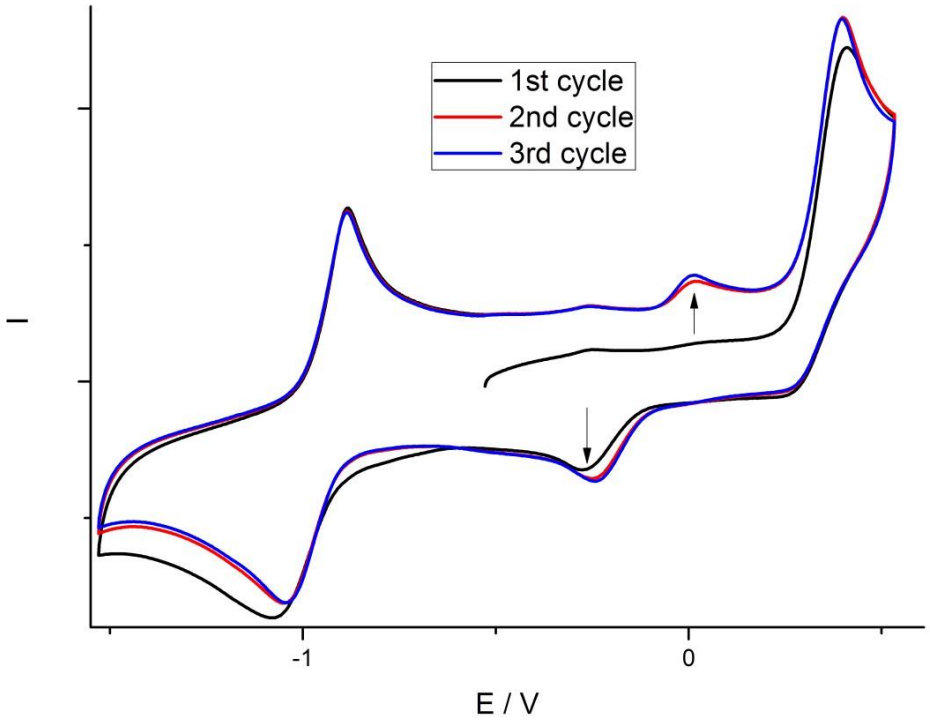

Figure S7: CV of compound **3** in a 1M $TBAPF_6$ solution of THF, the data was calibrated externally against $E_{1/2}(Fc/Fc^+)$.

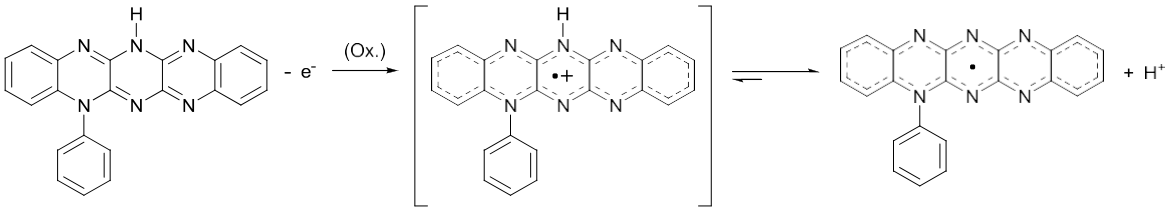

Scheme S1: Mechanism of the one electron oxidation reaction of **3**.

CV of the other species are depicted in Figure S8 (**3H**$^+$), Figure S9 (**3H**$_2^{2+}$) and Figure S10 (**3**$^-$), respectively.

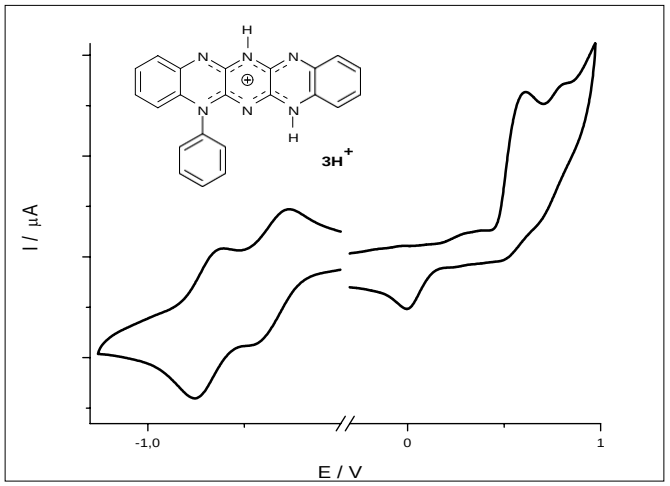

Figure S8: CV of the protonated species $\mathbf{3H^+}$.

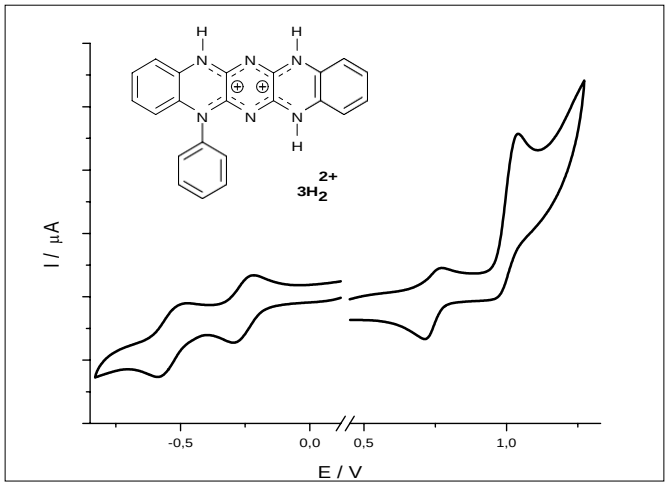

Figure S9: CV of the double protonated species $\mathbf{3H_2^{2+}}$.

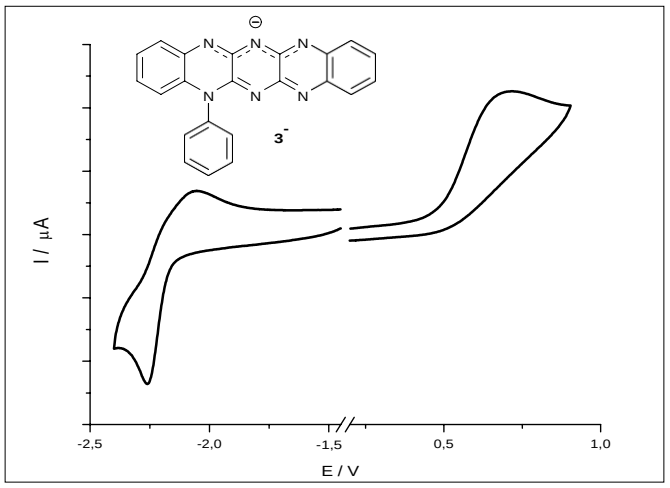

Figure S10: CV of the deprotonated species $\mathbf{3^-}$.

3 Computational Methods

3.1 Tautomerism / Absorption, Emission spectroscopy

To get a closer insight into the electronic structure of the studied molecule density functional theory (DFT) and time dependent density functional theory (TDDFT) were applied. The effects of solvation (MeOH) have been addressed for ground and excited state properties by means of a polarizable continuum model.[6] After an initial systematic conformational search with MMFF,[7] the best geometries were optimized at the B3LYP/6-31+G(d,p)[8] level of theory as implemented in Gaussian 09.[9] After the ground state optimization and its validation via frequency calculation, the six lowest singlet excited states have been calculated. Fluorescence emission was calculated according to Kasha[10] from the S1 equilibrium structure. The predicted ground-state structures are, expectedly, nearly perfectly planar. Only the aryl side unit is twisted with regard to the azaazene core of about 90°. In general the results are good agreement with the experimental values. Nonetheless, it must be emphasized that the calculated absorption properties entail a larger error than the calculated emission properties. Yet the error is mostly within the 0.3 eV margin that is typical of TD-DFT calculations.[11, 12]

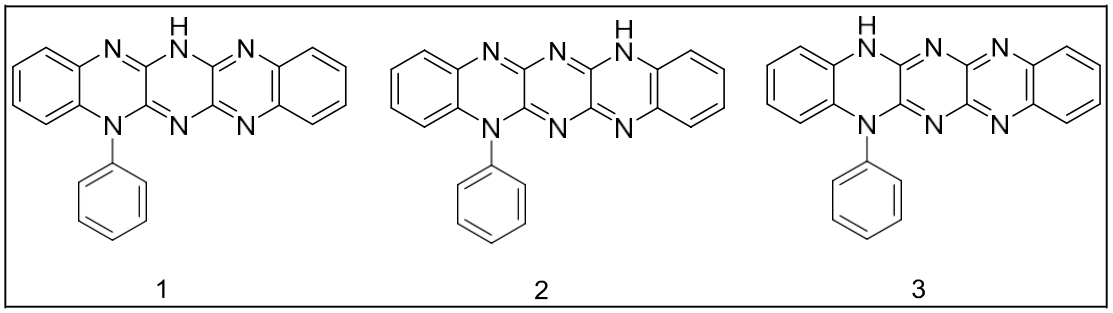

	E (hartree)	E (kJ/mol)	dE (kJ/mol)	Boltzmann Dist
1	-1174.76394890	-3084342.748	0.00	0.999707
2	-1174.75191213	-3084311.145	31.60	0.000003
3	-1174.75625934	-3084322.559	20.19	0.000290

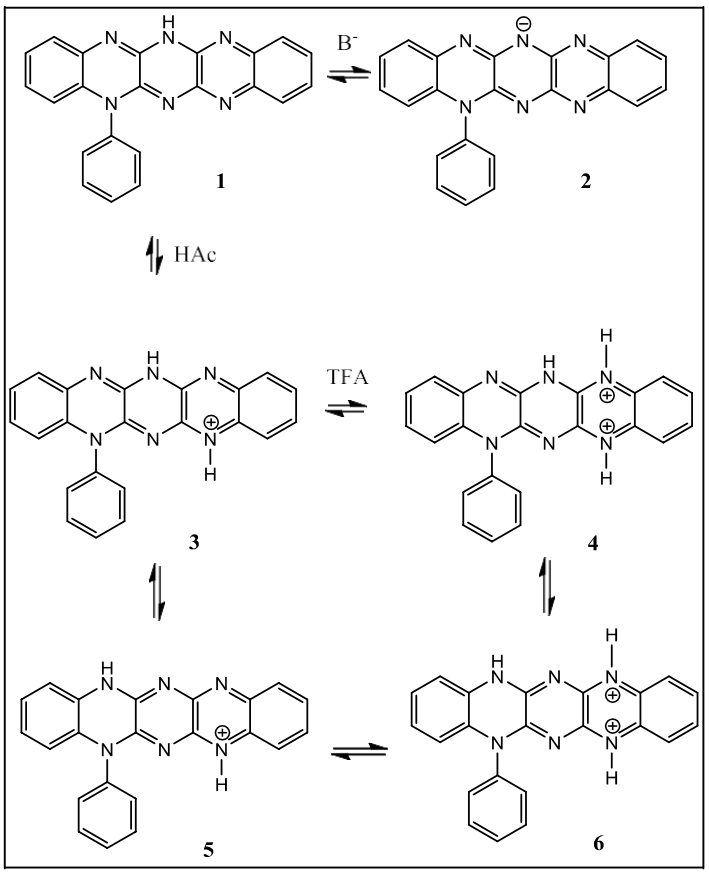

	E [Hartrees]	E [kJ/mol]
1 (≙ **3**)	-1174.78065	-3084386.6
2 (≙ **3**$^{-}$)	-1174.30501	-3083137.81
3 (≙ **3H**$^{+}$)	-1175.22314	-3085548.36
4	-1175.63589	-3086632.04
5	-1175.21895	-3085537.36
6 (≙ **3H**$_2^{2+}$)	-1175.64205	-3086648.19

	Emi [nm]	Emi [eV]	Error [eV]	Root Square Err
3	551.3	2.24922909	0.00691445	0.00691445
3^{-}	614.32	2.01849199	-0.15313673	0.15313673
3H^{+}	591.87	2.09505466	-0.11528402	0.11528402
3H$_2^{2+}$	670.91	1.84823598	-0.13894351	0.13894351

	Abs [nm]	Abs [eV]	Error [eV]	Root Square Err
3	443.84	2.79379957	2.79379957	2.79379957

3^{-}	495.02	2.50494929	2.50494929	2.50494929
3H^{+}	489	2.53578732	2.53578732	2.53578732
3H$_2^{2+}$	538.39	2.30316313	2.30316313	2.30316313

3.2 HOMO/LUMO Energies

B3LYP

	HOMO	LUMO	Error HOMO	Error LUMO
3	-5.65	-2.49	0.93	1.51
3^{-}	-4.72	-1.91	0.27	0.79
3H^{+}	-6.31	-3.46	0.24	0.84
3H$_2^{2+}$	-6.99	-4.58	-0.14	0.14
		average:	0.32	0.82

PBE

	HOMO	LUMO	Error HOMO	Error LUMO
3	-5.08	-3.04	1.50	0.96
3^{-}	-4.20	-2.43	0.79	0.27
3H^{+}	-5.75	-3.95	0.80	0.35
3H$_2^{2+}$	-6.45	-4.96	0.40	-0.24
		average:	0.88	0.34

PBE0

	HOMO	LUMO	Error HOMO	Error LUMO
3	-5.87	-2.41	0.71	1.59
3^{-}	-4.92	-1.83	0.07	0.87
3H^{+}	-6.53	-3.39	0.02	0.91
3H$_2^{2+}$	-7.20	-4.53	-0.35	0.19
		average:	0.11	0.89

B2PLYP

	HOMO	LUMO	Error HOMO	Error LUMO
3	-6.35	-1.19	0.23	2.81
3^{-}	-5.34	-0.66	-0.35	2.04
3H^{+}	-6.99	-2.23	-0.44	2.07
3H$_2^{2+}$	-7.64	-3.51	-0.79	1.21
		average:	-0.34	2.03

wB97XD

	HOMO	LUMO	Error	Error LUMO

			HOMO	
3	-7.37	-0.91	-0.79	3.09
$\mathbf{3}^-$	-6.36	-0.38	-1.37	2.32
$\mathbf{3H}^+$	-8.00	-1.94	-1.45	2.36
$\mathbf{3H_2}^{2+}$	-8.63	-3.18	-1.78	1.54
		average:	-1.35	2.33

CAM-B3LYP

	HOMO	LUMO	Error HOMO	Error LUMO
3	-6.83	-1.45	-0.25	2.55
$\mathbf{3}^-$	-5.83	-0.92	-0.84	1.78
$\mathbf{3H}^+$	-7.47	-2.48	-0.92	1.82
$\mathbf{3H_2}^{2+}$	-8.11	-3.71	-1.26	1.01
		average:	-0.81	1.79

PBE/PBE0

	HOMO	LUMO	Error HOMO	Error LUMO
3	-5.08	-2.41	1.50	1.59
$\mathbf{3}^-$	-4.20	-1.83	0.79	0.87
$\mathbf{3H}^+$	-5.75	-3.39	0.80	0.91
$\mathbf{3H_2}^{2+}$	-6.45	-4.53	0.40	0.19
		average:	0.88	0.89

4 Attachment

4.1 Single crystal X-Ray data of compound 3

Crystal Data for $\mathbf{3H_2}^{2+}$***2Cl**$^{-}$: $C_{22}H_{16}Cl_2N_6$, Mr = 435.31 gmol^{-1}, red prism, size 0.134 x 0.122 x 0.112 mm^3, monoclinic, space group P $2_1/c$, a = 11.6748(3), b = 10.2522(3), c = 16.7835(5) Å, β = 103.528(1)°, V = 1953.12(10) Å^3, T= -140 °C, Z = 4, $\rho_{calcd.}$ = 1.480 gcm^{-3}, μ (Mo-K_α) = 3.56 cm^{-1}, multi-scan, transmin: 0.7005, transmax: 0.7456, F(000) = 896, 13792 reflections in h(-15/15), k(-12/13), l(-21/21), measured in the range 1.79° ≤ Θ ≤ 27.42°, completeness Θ_{max} = 99.4%, 4428 independent reflections, R_{int} = 0.0442, 3737 reflections with $F_o > 4\sigma(F_o)$, 335 parameters, 0 restraints, $R1_{obs}$ = 0.0448, wR^2_{obs} = 0.0988, $R1_{all}$ = 0.0575, wR^2_{all} = 0.1055, GOOF = 1.117, largest difference peak and hole: 0.358 / -0.295 e Å^{-3}.

Supporting Information Available: Crystallographic data deposited at the Cambridge Crystallographic Data Centre under CCDC-1497236 for $\mathbf{3H_2^{2+}*2Cl^-}$ contain the supplementary crystallographic data excluding structure factors; this data can be obtained free of charge via www.ccdc.cam.ac.uk/conts/retrieving.html (or from the Cambridge Crystallographic Data Centre, 12, Union Road, Cambridge CB2 1EZ, UK; fax: (+44) 1223-336-033; or deposit@ccdc.cam.ac.uk).

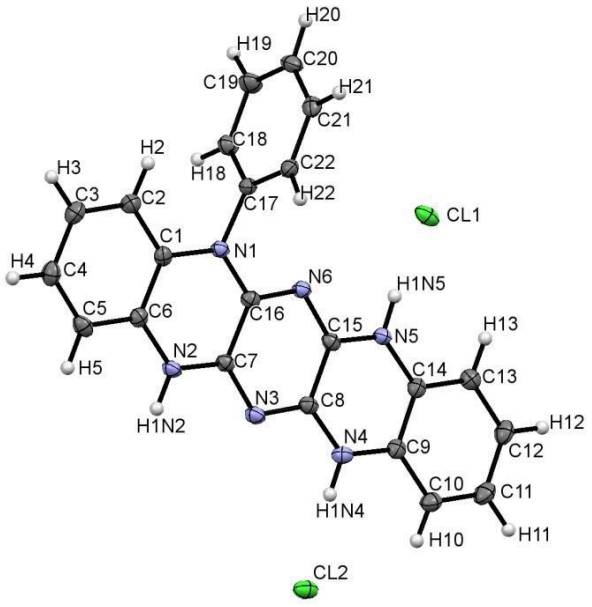

Figure S11: ORTEP view of $\mathbf{3H_2}^{2+}$ 2Cl$^-$, showing the atom numbering scheme. The ellipsoids represent a probability of 30 %.

4.2 NMR spectra

^{1}H-NMR:

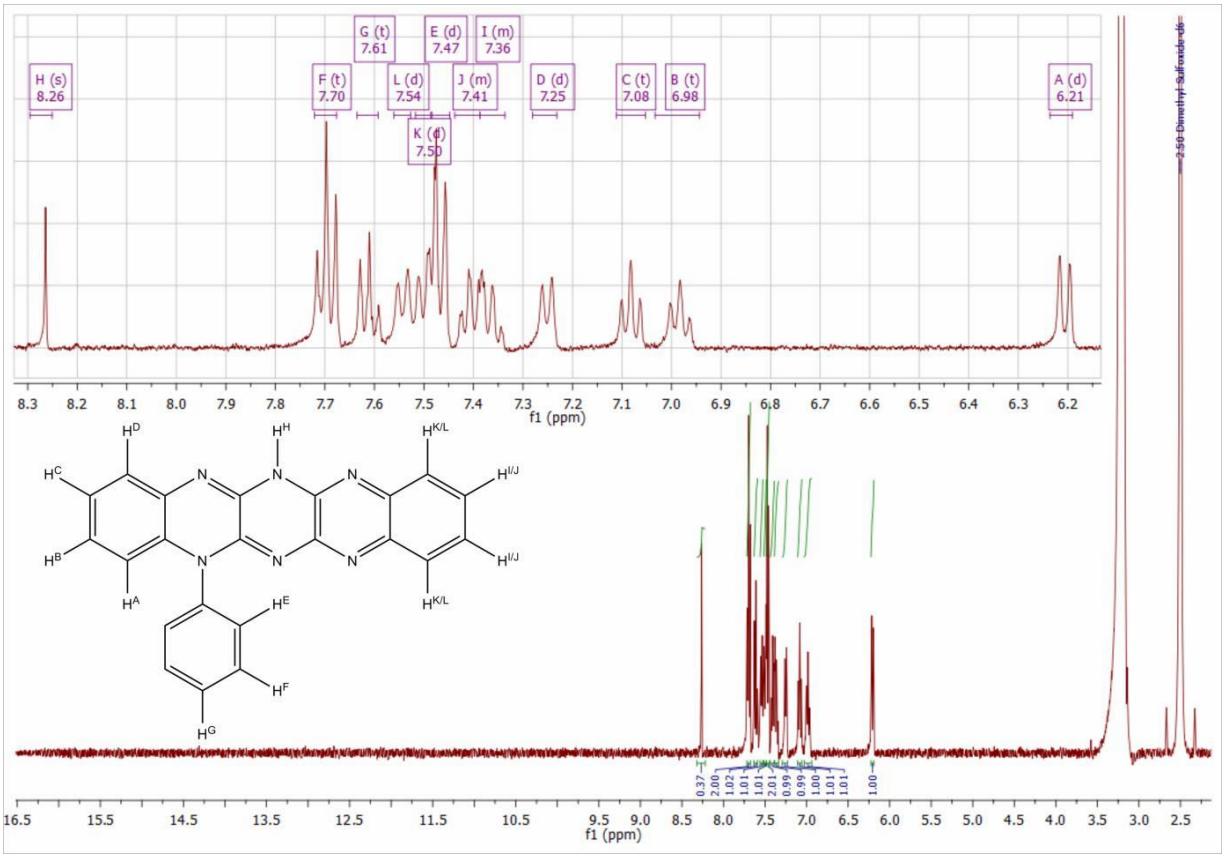

^{1}H-^{1}H-Cosy:

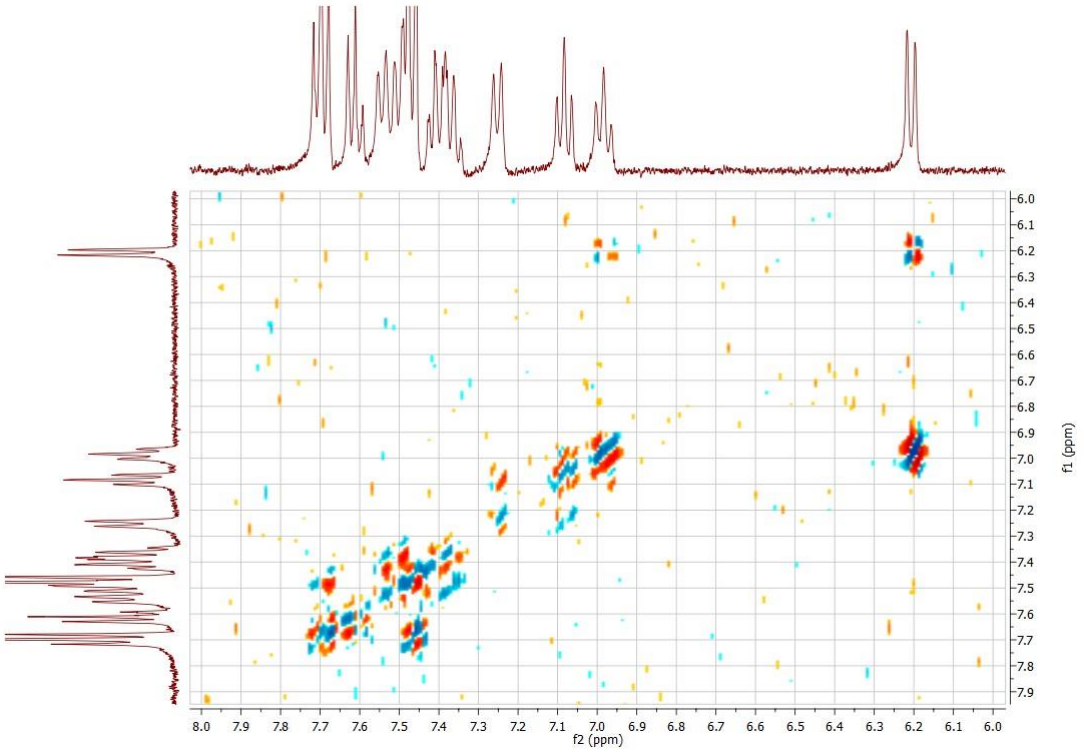

^{13}C-NMR:

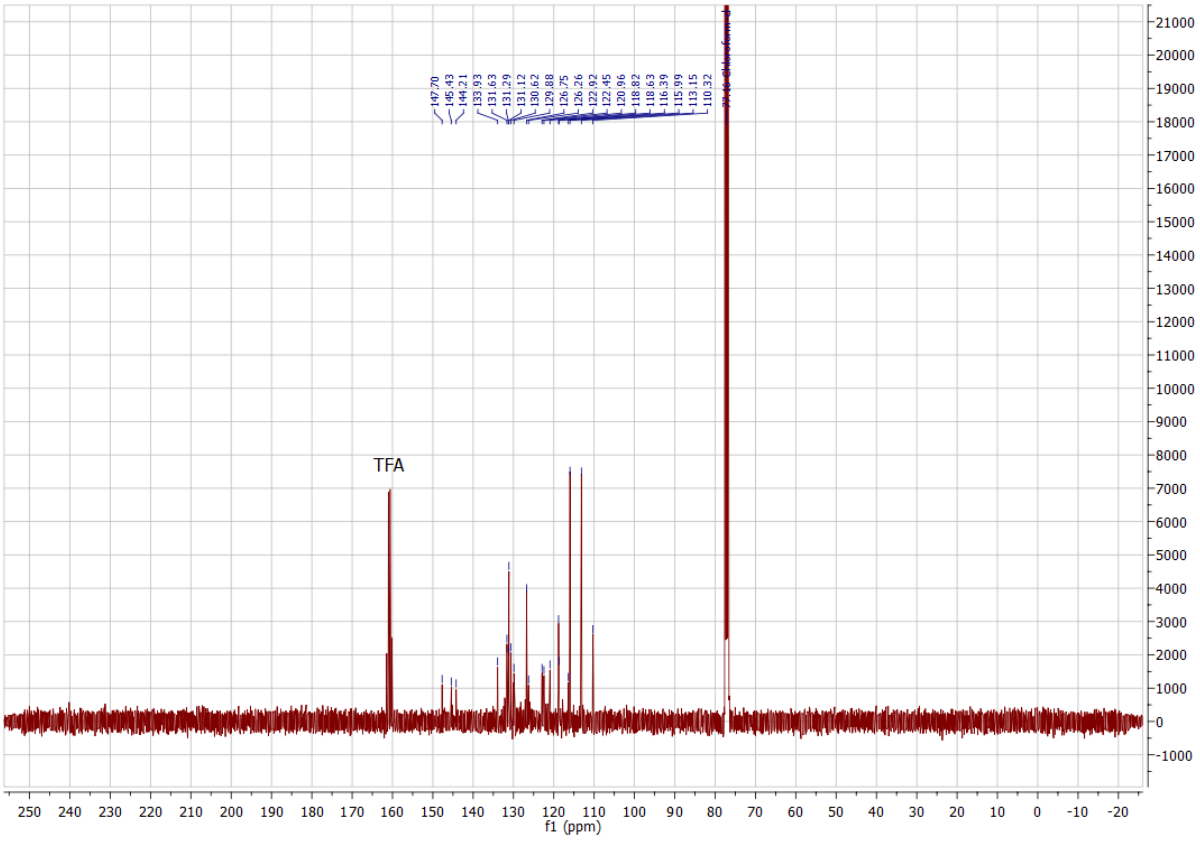

5 Literature

[1] a) COLLECT, Data Collection Software, R. Hooft, Nonius BV, Delft, The Netherlands, 1998; b) Z. Otwinowski and W. Minor, *Methods Enzymol.*, 1997, **276** (Ed.: Charles W. Carter Jr.), Academic Press, 307–326; c) SADABS 2.10, Bruker-AXS inc., 2002, Madison, WI, U.S.A.

[2] G. Sheldrick, *Acta Crystallogr., Sect. A*, 2008, **64**, 112–122.

[3] MERCURY, C. F. Macrae, P. R. Edgington, P. McCabe, E. Pidcock, G. P. Shields, R. Taylor, M. Towler and J. van de Streek, *J. Appl. Cryst.*, 2006, **39**, 453.

[4] (a) A. M. Brouwer, *Pure Appl. Chem.*, 2011, **83**; (b) S. Fery-Forgues and D. Lavabre, , *J. Chem. Educ.*, 1999, **76**, 1260.

[5] K. J. L. Sawtschenko, A. Neudeck and L. Dunsch, *Electrochim. Acta*, 1996, **41**, 123-131.

[6] J. Tomasi, B. Mennucci and R. Cammi, *Chem. Rev.*, 2005, **105**, 2999.

[7] T. A. Halgren, *J. Comput. Chem.*, 1996, **17**, 490.

[8] T. Yanai, D. P. Tew and N. C. Handy, *Chem. Phys. Lett.*, 2004, **393**, 51.

[9] M. J. Frisch, G. W. Trucks, H. B. Schlegel, G. E. Scuseria, M. A. Robb, J. R. Cheeseman, G. Scalmani, V. Barone, B. Mennucci, G. A. Petersson, H. Nakatsuji, M. Caricato, X. Li, H. P. Hratchian, A. F. Izmaylov, J. Bloino, G. Zheng, J. L. Sonnenberg, M. Hada, M. Ehara, K. Toyota, R. Fukuda, J. Hasegawa, M. Ishida, T. Nakajima, Y. Honda, O. Kitao, H. Nakai, T. Vreven, J. A. Montgomery Jr., J. E. Peralta, F. Ogliaro, M. Bearpark, J. J. Heyd, E. Brothers, K. N. Kudin, V. N. Staroverov, R. Kobayashi, J. Normand, K. Raghavachari, A. Rendell, J. C. Burant, S. S. Iyengar, J. Tomasi, M. Cossi, N. Rega, M. J. Millam, M. Klene, J. E. Knox, J. B. Cross, V. Bakken, C. Adamo, J. Jaramillo, R. Gomperts, R. E. Stratmann, O. Yazyev, A. J. Austin, R. Cammi, C. Pomelli, J. W. Ochterski, R. L. Martin, K. Morokuma, V. G. Zakrzewski, G. A. Voth, P. Salvador, J. J. Dannenberg, S. Dapprich, A. D. Daniels, Ö. Farkas, J. B. Foresman, J. V. Ortiz, J. Cioslowski and D. J. Fox, Gaussian 09, Revision A.02, Gaussian, Inc., Wallingford, CT, 2009.

[10] a) D. Jacquemin, V. Wathelet, E. A. Perpète and C. Adamo, *J. Chem. Theory Comput.*, 2009, **5**, 2420; b) D. Jacquemin, E. Perpète, I. Ciofini and C. Adamo, *Theor. Chem. Acc.*, 2011, **128**, 127.

[11] L. Pinto da Silva and J. C. G. Esteves da Silva, *Int. J. Quantum Chem.*, 2013, **113**, 45.

[12] M. Kasha, *Discuss. Faraday Soc.*, 1950, **9**, 14–19.